SEPSIS

Interleukin-3 amplifies acute inflammation and is a potential therapeutic target in sepsis

Georg F. Weber,[1,2]*† Benjamin G. Chousterman,[1]* Shun He,[1]* Ashley M. Fenn,[1] Manfred Nairz,[1] Atsushi Anzai,[1] Thorsten Brenner,[3] Florian Uhle,[3] Yoshiko Iwamoto,[1] Clinton S. Robbins,[1] Lorette Noiret,[1] Sarah L. Maier,[2] Tina Zönnchen,[2] Nuh N. Rahbari,[2] Sebastian Schölch,[2] Anne Klotzsche-von Ameln,[4] Triantafyllos Chavakis,[4] Jürgen Weitz,[2] Stefan Hofer,[3] Markus A. Weigand,[3] Matthias Nahrendorf,[1] Ralph Weissleder,[1,5] Filip K. Swirski[1]*†

Sepsis is a frequently fatal condition characterized by an uncontrolled and harmful host reaction to microbial infection. Despite the prevalence and severity of sepsis, we lack a fundamental grasp of its pathophysiology. Here we report that the cytokine interleukin-3 (IL-3) potentiates inflammation in sepsis. Using a mouse model of abdominal sepsis, we showed that innate response activator B cells produce IL-3, which induces myelopoiesis of Ly-6C^{high} monocytes and neutrophils and fuels a cytokine storm. IL-3 deficiency protects mice against sepsis. In humans with sepsis, high plasma IL-3 levels are associated with high mortality even after adjusting for prognostic indicators. This study deepens our understanding of immune activation, identifies IL-3 as an orchestrator of emergency myelopoiesis, and reveals a new therapeutic target for treating sepsis.

Interleukin-3 (IL-3) contributes to leukocyte production, proliferation, and survival (*1*–*4*). Myeloid cells such as monocytes and neutrophils produce IL-1β, IL-6, and tumor necrosis factor–α (TNF-α), the three inflammatory hallmark cytokines constituting the cytokine storm during septic shock (*5*–*7*). Yet despite these links, IL-3's role in sepsis remains unknown. *Il3*$^{-/-}$ mice have normal blood monocyte and neutrophil profiles (fig. S1, A to G) (*8*) and thus do not require IL-3 for myelopoiesis in the steady state. To test whether IL-3 is important in sepsis, we subjected *Il3*$^{-/-}$ and control wild-type (WT) mice to cecal ligation and puncture (CLP), a model of polymicrobial sepsis (*9*). Compared to WT mice, *Il3*$^{-/-}$ mice were protected from sepsis, as seen in their lower mortality rates, even after antibiotic treatment (Fig. 1A). *Il3*$^{-/-}$ mice had better clinical scores, body temperatures (Fig. 1B), and blood pressure (Fig. 1C), and their recovery was associated with efficient microbial clearance, indicating that the absence of IL-3 did not compromise bactericidal activity or recognition (Fig. 1D and fig. S2).

To characterize the host response more completely, we performed time-course tissue, cellular, and molecular experiments. At 1 day after CLP, WT mice developed neutrophilia and inflammatory Ly-6C^{high} monocytosis (Fig. 1E), whereas in *Il3*$^{-/-}$ mice, monocyte and neutrophil numbers remained relatively unchanged. The increased cell numbers in WT mice were associated with higher serum levels of IL-1β, IL-6, and TNF-α (Fig. 1F). Phagocytic leukocytes were major sources of IL-1β, IL-6, and TN-Fα, because phagocyte depletion with clodronate liposomes and anti–Ly-6G before CLP abolished the cytokine storm (fig. S3A). However, IL-3–mediated cytokine induction was indirect: Both WT and *Il3*$^{-/-}$ neutrophils and monocytes contained similar intracellular reservoirs of the three cytokines (fig. S3B). Analyzing other leukocytes showed IL-3–dependent differences in T and B cell numbers after CLP (fig. S4A), but no differences in basophils, mast cells (*10*–*12*) (fig. S4, B and C), or histamine (fig. S4D), which suggests that IL-3 had little to no effect on basophil and mast cell production and function during the initial inflammation-dominant phase. Consequently, WT but not *Il3*$^{-/-}$ mice accumulated monocytes and neutrophils in the lung (Fig. 1G) and liver (Fig. 1H); developed lung pathology (fig. S5A) with increased protein in bronchoalveolar lavage (fig. S5B); and evolved abnormal liver morphology (fig. S5C) with increased markers of cytolysis in serum (fig. S5D). These data show that IL-3 contributed to septic shock, the most severe form of sepsis (*13*, *14*).

IL-3 promotes hematopoiesis by acting on its receptor, a heterodimer that consists of the IL-3–specific α chain (CD123) and the common β chain (CD131) (*4*). In the steady state, Lin$^-$ c-kit$^+$ hematopoietic stem and progenitor cells (HSPCs), including megakaryocyte and erythrocyte progenitors (MEPs), common myeloid progenitors (CMPs), granulocyte and macrophage progenitors (GMPs), and macrophage and dendritic progenitors (MDPs), expressed CD123 at the same level in both WT and *Il3*$^{-/-}$ mice (Fig. 2A and S6). One day after CLP, the numbers of medullary HSPCs, CMPs, MEPs, and GMPs/MDPs increased over the steady state in WT but not *Il3*$^{-/-}$ mice (Fig. 2B). GMPs are committed to differentiate into monocytes and neutrophils (*15*). We therefore pursued fate-mapping experiments involving adoptively transferring green fluorescent protein–positive (GFP$^+$) GMPs into WT or *Il3*$^{-/-}$ mice. In response to CLP, the bone marrow of WT mice contained a larger population of GFP$^+$ cells than the bone marrow of *Il3*$^{-/-}$ mice, indicating IL-3–dependent progenitor expansion (Fig. 2C). To bolster this observation, we placed Lin$^-$ bone marrow cells (containing predominantly HSPCs) in vitro in medium either alone or supplemented with IL-3, lipopolysaccharide (LPS), or both. We found that IL-3, but not LPS, increased cell expansion and generated myeloid cells well above the numbers initially placed into culture (Fig. 2D). Although IL-3 alone modestly affected IL-1β, IL-6, and TNF-α production, combined IL-3 and LPS exacerbated the response (Fig. 2E). These data suggest that IL-3 is responsible for the cytokine storm, albeit indirectly, by generating a large pool of cells that, upon recognizing bacterial components, produce cytokines in larger quantities.

To determine whether IL-3 can trigger severe sepsis in vivo, whether it can do so alone or in combination with infection, and whether it relies on its specific receptor, we injected (i) recombinant IL-3 (rIL-3) into otherwise healthy WT mice; (ii) anti-CD123 into WT mice subjected to CLP; and (iii) rIL-3 into *Il3*$^{-/-}$ mice subjected to CLP. rIL-3 augmented GMPs in the bone marrow and leukocyte numbers in the blood of healthy WT mice to levels akin to those in WT mice subjected to CLP (Fig. 2F). Despite this increase, rIL-3 per se did not induce a cytokine storm in the absence of infection (Fig. 2G), thus confirming our in vitro observations. Conversely, anti-CD123 attenuated cell numbers in WT CLP mice (Fig. 2F) and tended to decrease serum cytokines (although the differences were not statistically significant) (Fig. 2G) without depleting HSPCs (fig. S7). *Il3*$^{-/-}$ mice receiving rIL-3 in the context of CLP augmented medullary GMP, circulating neutrophil, and Ly-6C^{high} monocyte numbers (Fig. 2F). These increases corresponded to higher cytokine levels in serum (Fig. 2G). Ultimately, WT mice treated with anti-CD123 had a modest but significant improvement in survival (Fig. 2H), whereas *Il3*$^{-/-}$ mice receiving rIL-3 succumbed to infection and died as often as WT mice (Fig. 2I). These data confirm the effects of IL-3 on cell production and survival and identify the IL-3–CD123 axis as a potential new therapeutic target for treating sepsis.

Activated T cells (*16*) and thymic epithelial cells (*17*) produce IL-3 in the steady state, but the

[1]Center for Systems Biology, Massachusetts General Hospital, Harvard Medical School, Boston, MA, USA. [2]Department of Visceral, Thoracic and Vascular Surgery, Technische Universität Dresden, Dresden, Germany. [3]Department of Anesthesiology, University of Heidelberg, Heidelberg, Germany. [4]Department of Clinical Pathobiochemistry and Institute for Clinical Chemistry and Laboratory Medicine, Technische Universität Dresden, Dresden, Germany. [5]Department of Systems Biology, Harvard Medical School, Boston, MA 02115, USA.
*These authors contributed equally to this work.
†Corresponding author. E-mail: fswirski@mgh.harvard.edu (F.K.S.); georg.weber@uniklinikum-dresden.de (G.F.W.)

cytokine's source in sepsis is unknown. mRNA profiling identified the spleen, thymus, and lymph nodes as hubs of basal *Il3* expression. After CLP, *Il3* mRNA progressively increased in the spleen, followed by the thymus and lymph nodes, with no signal in the bone marrow, lung, liver, peritoneum, or duodenum (Fig. 3A). As indicated by flow cytometry (Fig. 3, B and C) and Western blots (Fig. 3D), IL-3$^+$ cells were CD19$^+$ B cells. According to enzyme-linked immunosorbent assay, IL-3 levels increased in serum after CLP (Fig. 3E) but to a lesser extent in splenectomized mice (Fig. 3E).

Identifying B cells as sources of IL-3 prompted testing of whether IL-3–producing B cells resemble innate response activator (IRA) B cells (fig. S8A), whose GM-CSF (granulocyte-macrophage colony-stimulating factor) product protects against sepsis and pneumonia via polyreactive immunoglobulin M (IgM) (*18*, *19*). Phenotypic profiling showed that splenic IL-3 producers were IgM^{high} CD23^{low} CD19$^+$ CD138^{high} CD43$^+$ VLA4$^+$ (Fig. 3F and fig. S8B), as well as CD5^{int} LFA1$^+$ CD284$^+$ CD11b$^{low/-}$ (fig. S8C). This phenotype matches that of IRA

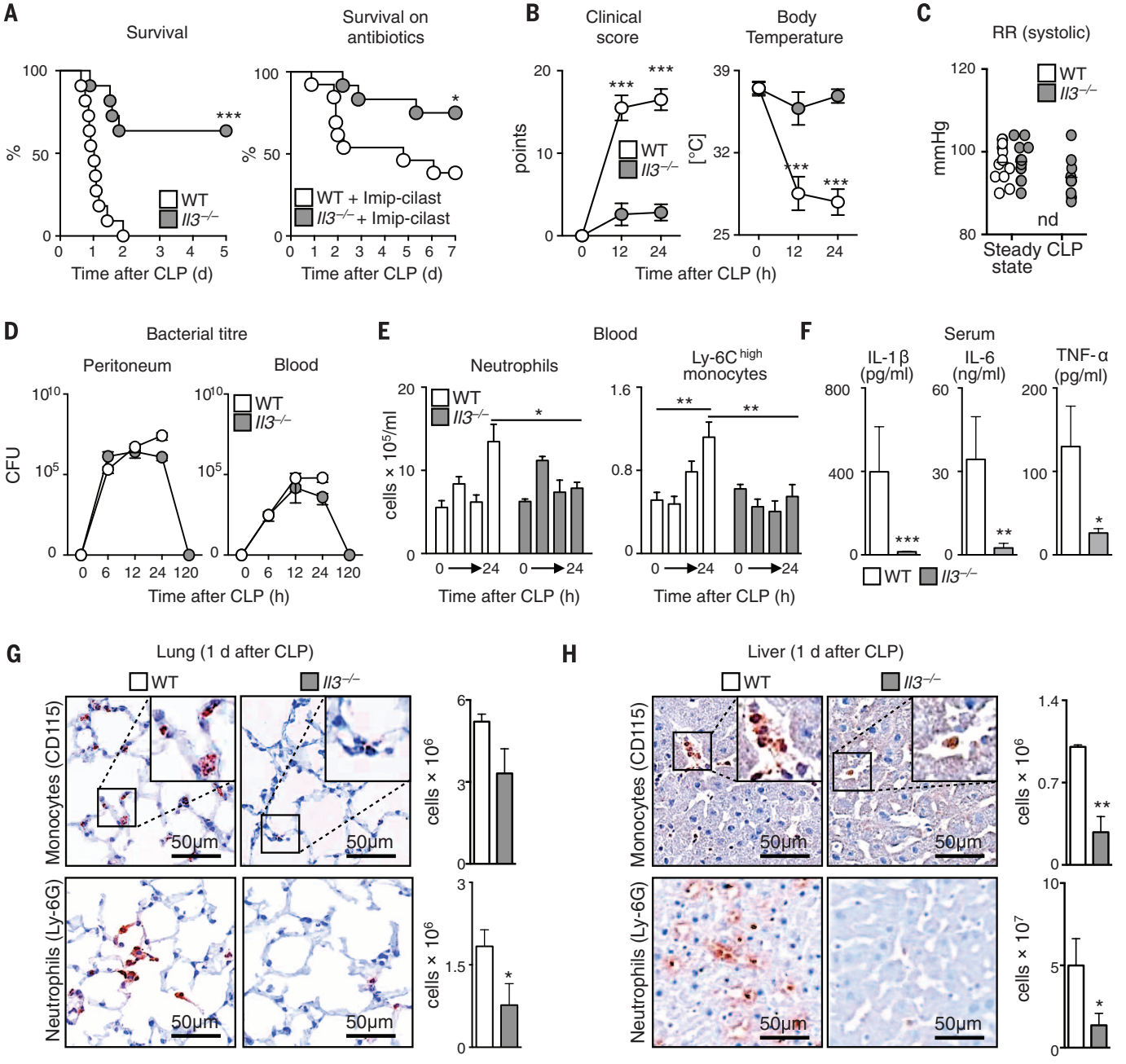

Fig. 1. IL-3 is detrimental in experimental sepsis. Comparison of *Il3*$^{-/-}$ and Balb/c (WT) mice during experimental sepsis using the CLP model. (**A**) Kaplan-Meier survival curve in mice not receiving antibiotics (n = 10 mice per group) and in mice receiving antibiotics (Imipenem) (n = 12 or 13 per group). d, days. (**B**) Clinical score and body temperature (n = 6 to 10 per group). h, hours. (**C**) Blood pressure. The blood pressure in WT mice was below the detection limit (n = 6 to 10 per group). (**D**) Bacterial titer of peritoneal cavity and blood (n = 3 to 10 per group). (**E**) Enumeration of neutrophils and Ly-6C^{high} monocytes in 1 ml of blood at 0, 6, 12, and 24 hours after CLP (n = 3 to 12 per group). (**F**) Levels of IL-1β, IL-6, and TNF-α in serum 1 day after CLP (n = 8 or 9 per group). (**G** and **H**) Immunohistochemical staining and flow cytometric enumeration of monocytes (CD115) and neutrophils (Ly-6G) in entire lung (G) and liver (H) tissue 1 day after CLP (n = 6; *P < 0.05, **P < 0.01, ***P < 0.001). Error bars indicate means ± SEM. Significance was assessed by log rank test (A) or Mann-Whitney test [(B) to (H)]. Data are the result of $N \geq 2$ independent experiments and are grouped.

B cells (*18*–*20*). The remaining, non-B IL-3–positive cells in the spleen and thymus were $CD4^+$ T cells, $CD8^+$ T cells, and non-T, non-B cells (fig. S8D).

By comparing IL-3 and GM-CSF, which are two IRA B cell products, we determined that the growth factors are not interdependent: In response to CLP, the spleens of *Csf2*$^{-/-}$ mice accumulated IL-3–producing IRA B cells, whereas *Il3*$^{-/-}$ mice accumulated GM-CSF–producing IRA B cells (fig. S9A). On the one hand, in contrast to GM-CSF (*19*), IL-3 was not essential to IgM production (fig. S9, B and C). On the other hand, unlike IL-3, GM-CSF was dispensable for emergency myelopoiesis (fig. S9D, E). The IL-3–producing IRA B cells were readily visualized by immunofluorescence and increased in frequency after CLP (Fig. 3, G and H, and fig. S10). Thus, IRA B cells can both protect against and aggravate sepsis, depending on the particular growth factor they produce.

Peritoneal B1 cells relocate to the spleen after peritoneal LPS challenge (*21*) and differentiate to IRA B cells (*18*). To determine whether IL-3$^+$ B cells arise similarly, we transferred B1 cells from the peritoneum of naïve GFP^+ mice into the peritoneum of WT mice. Two days after CLP, IL-3$^+$ (Fig. 3I) and $GM\text{-}CSF^+$ B cells (fig. S11) accumulated in the spleen, indicating peritoneal B cell relocation, splenic accumulation, and IRA B cell differentiation. To test whether IL-3–producing B cells are important in sepsis, we transferred peritoneal B1 B cells from WT or *Il3*$^{-/-}$ mice into *Il3*$^{-/-}$ mice subjected to CLP and found increased monocyte levels, cytokine levels, and morbidity in WT B cell recipients (Fig. 3J). Overall, the data show that IL-3–producing IRA B cells induce emergency myelopoiesis and potentiate septic shock in a mouse sepsis model.

Because the validity of mouse sepsis models as mirrors of human disease has been challenged (*22*, *23*), we sought to determine whether our experimental findings correlate with the pathogenesis of human sepsis. First, we retrospectively analyzed plasma from a cohort of septic patients [RAMMSES cohort, $n = 60$ (table S1)] (*24*) and found that IL-3 levels during the first 24 hours after the onset of sepsis predicted death: Patients

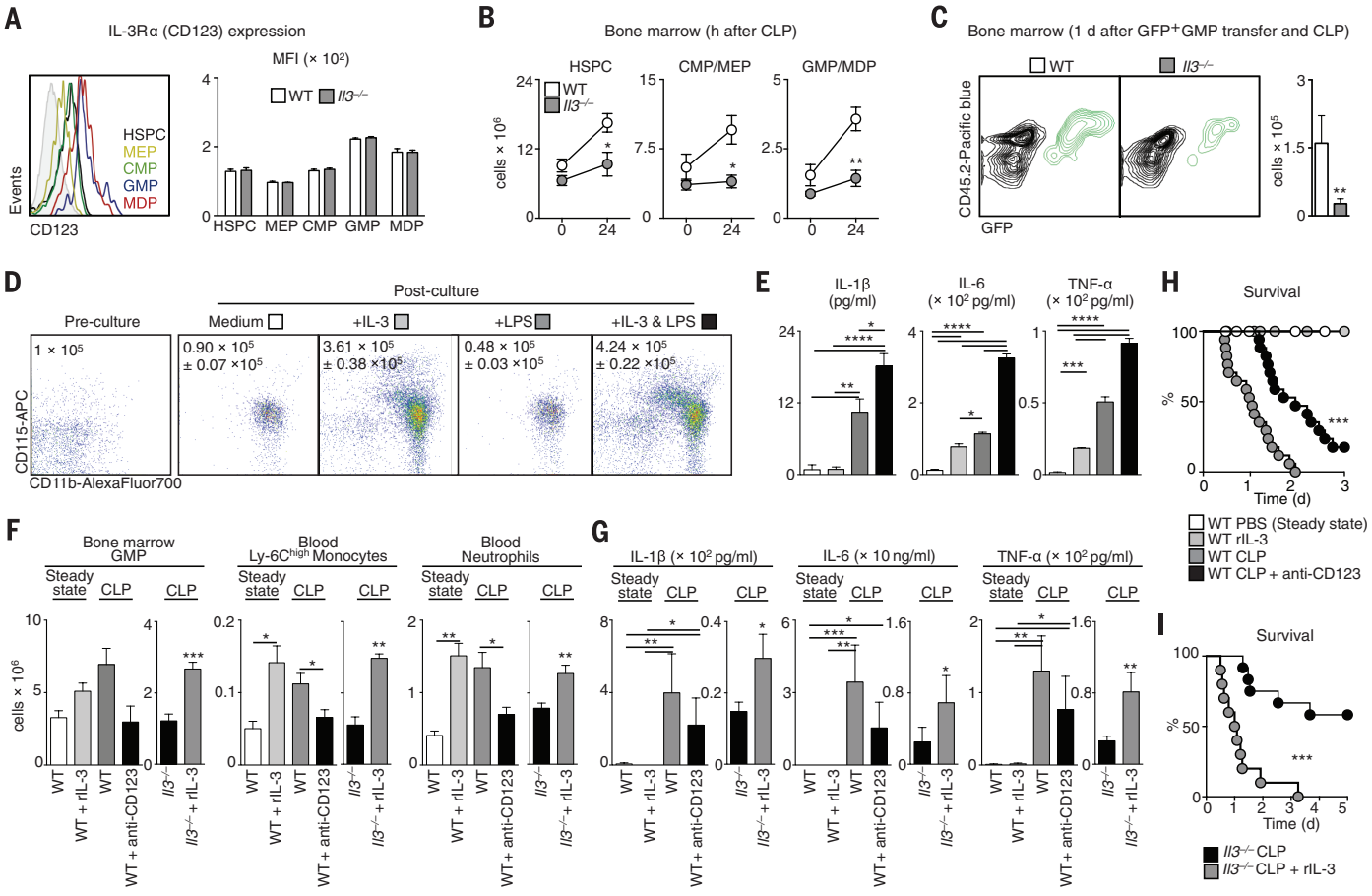

Fig. 2. IL-3 induces emergency hematopoiesis and potentiates the cytokine storm in sepsis. (**A**) Surface expression of IL-3Rα (CD123) on HSPCs, MEPs, CMPs, GMPs, and MDPs in bone marrow of WT and *Il3*$^{-/-}$ mice ($n = 3$ per group). A representative plot of $n = 3$ is shown. (**B**) Enumeration of HSPCs, CMPs/MEPs, and GMPs/MDPs in bone marrow in a steady state and 1 day after CLP in WT and *Il3*$^{-/-}$ mice ($n = 3$ per group). (**C**) Analysis and enumeration of GFP^+ cells retrieved from the bone marrow 1 day after CLP from WT and *Il3*$^{-/-}$ mice that received 2×10^5 GFP^+ GMP intravenously before CLP ($n = 3$ per group). (**D**) Bone marrow cells were sorted for Lin^- cells (i.e., enriched in HSPCs). Shown are representative CD11b versus CD115 flow cytometry plots showing cell phenotype just before placement into culture and 4 days after in vitro culture in the indicated conditions. The numbers inside the plots denote cells plated and retrieved ($n = 4$ per group). (**E**) Supernatant levels of IL-1β, IL-6, and TNF-α in the four post-culture groups shown in (D). Values are the result of technical triplicates from $n = 2$ experiments. (**F**) Enumeration of indicated cell types in (i) WT mice at a steady state; (ii) WT mice receiving rIL-3 alone; (iii) WT mice subjected to CLP; (iv) WT mice subjected to CLP and receiving antibody to CD123; (v) *Il3*$^{-/-}$ mice subjected to CLP; and (vi) *Il3*$^{-/-}$ mice subjected to CLP and receiving rIL-3 ($n = 4$ to 10). (**G**) Serum levels of IL-1β, IL-6, and TNF-α in the six groups shown in (F) ($n = 4$ to 10). (**H**) Kaplan-Meier survival curves showing the four WT mouse groups ($n = 6$ to 17 per group). (**I**) Kaplan-Meier survival curves showing the two *Il3*$^{-/-}$ mouse groups ($n = 10$ per group) (*$P < 0.05$, **$P < 0.01$, ***$P < 0.001$). Error bars indicate means ± SEM. Significance was assessed by Mann-Whitney test [(B), (C), (F), and (G)]; one-way analysis of variance (ANOVA) with Tukey's multiple comparison test (E); Kruskal-Wallis test with Dunn's multiple comparison test [(F) and (G)]; and log rank [(H) and (I)]. Data are the result of $N = 2$ independent experiments acquired in triplicates (in vitro) and $n \geq 2$ independent experiments (in vivo), and are grouped.

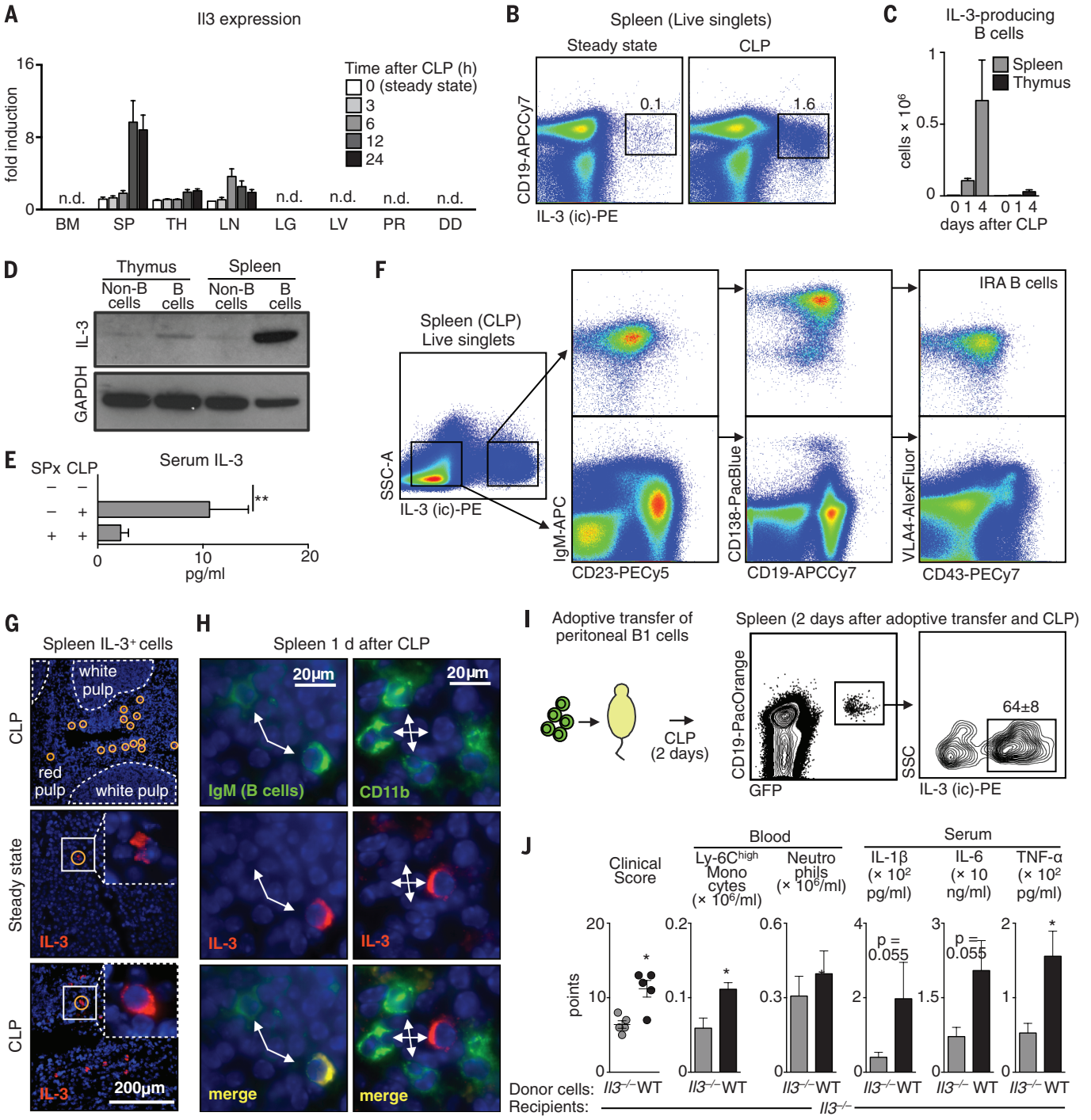

Fig. 3. IRA B cells are major sources of IL-3 in sepsis. (**A**) *Il3* mRNA expression in the indicated organs during a steady state and 3, 6, 12, and 24 hours after CLP (n = 6 to 8). (**B**) Identification of IL-3–producing cells in the spleen 4 days after CLP. (**C**) Enumeration of IL-3–producing B cells in spleen and thymus in a steady state and 1 and 4 days after CLP (n = 5). (**D**) Western blot showing IL-3 expression by B cells and non-B cells sorted from the spleen and thymus 1 day after CLP. (**E**) IL-3 serum levels in a steady state and 1 day after CLP with and without splenectomy (SPx) (n = 3 to 6). (**F**) Flow cytometric plots show the phenotype of IL-3$^+$ and IL-3$^-$ cells retrieved from the spleen after CLP. A representative plot of n = 5 is shown. (**G**) Immunofluorescence microscopy of spleen tissue in the steady state and 1 day after CLP. (**H**) Co-staining of representative IL-3$^+$ cells with IgM. (**I**) Adoptive transfer of 1.5 × 10^6 peritoneal B1 B cells from GFP$^+$ mice into WT mice subjected to CLP at the time of cell transfer. Representative plots from flow cytometric analysis of n = 3 mice are shown. (**J**) Adoptive transfer of 3 × 10^6 peritoneal B1 B cells from WT or *Il3*$^{-/-}$ mice to the peritoneum of *Il3*$^{-/-}$ recipients subjected to CLP. Data show the clinical score, number of Ly-6C^{high} monocytes, neutrophils, and serum cytokines 1 day after CLP (n = 5). (*P < 0.05, **P < 0.01). Error bars indicate means ± SEM. Significance was assessed by a Kruskal-Wallis test with Dunn's multiple comparison test (E) and a Mann-Whitney test (J).

with IL-3 plasma levels >87.4 pg/ml at admission had a poor prognosis (fig. S12, A and B, and table S2). We therefore decided to test, in a new prospective cohort [SEPIL-3 cohort, n = 37 (table S3)], whether IL-3 and blood monocytes correlate. In septic patients monitored over 28 days, blood leukocyte numbers peaked at the onset of sepsis and decreased slowly thereafter (Fig. 4A). The increase was associated with a sharp spike of plasma cytokines (Fig. 4B). Compared to healthy volunteers, mean IL-3 in septic patient plasma did not differ (Fig. 4C). Nevertheless, the detectable levels of IL-3 correlated with circulating monocyte levels in septic patients (Fig. 4D). Kaplan-Meier survival analysis showed that patients with plasma levels of >89.4 pg/ml had a poor prognosis (fig. S13 and table S4), thus confirming the results from the RAMMSES cohort. Pooling the cohorts showed the impact of IL-3 on survival to be even more striking (odds ratio: 4.979; confidence interval: 1.680 to 14.738 and P = 0.001 for the Kaplan-Meier survival curve) (Fig. 4E). The association remained significant after adjusting for prognostic parameters in multivariate analyses (table S5), whereas multivariate logistic regression analyses consistently showed improvement in the death prediction when IL-3 was included, as shown by a reduction of the Aikake information criterion and an increase of McFadden's pseudo R^2 (table S6). We also conducted flow cytometry and immunofluorescence on human spleens from patients undergoing splenectomy. By flow cytometry, we found CD20$^+$ HLADR^{int} CD19^{high} IgM$^{int/high}$ B and CD3$^+$ T cells to be producers of IL-3 (Fig. 4F and fig. S14A). In tissue sections, human spleens contained IL-3–producing CD19$^+$ and IgM$^+$ B cells (Fig. 4G and fig. S14, B and C), suggesting that IL-3–producing IRA B cells

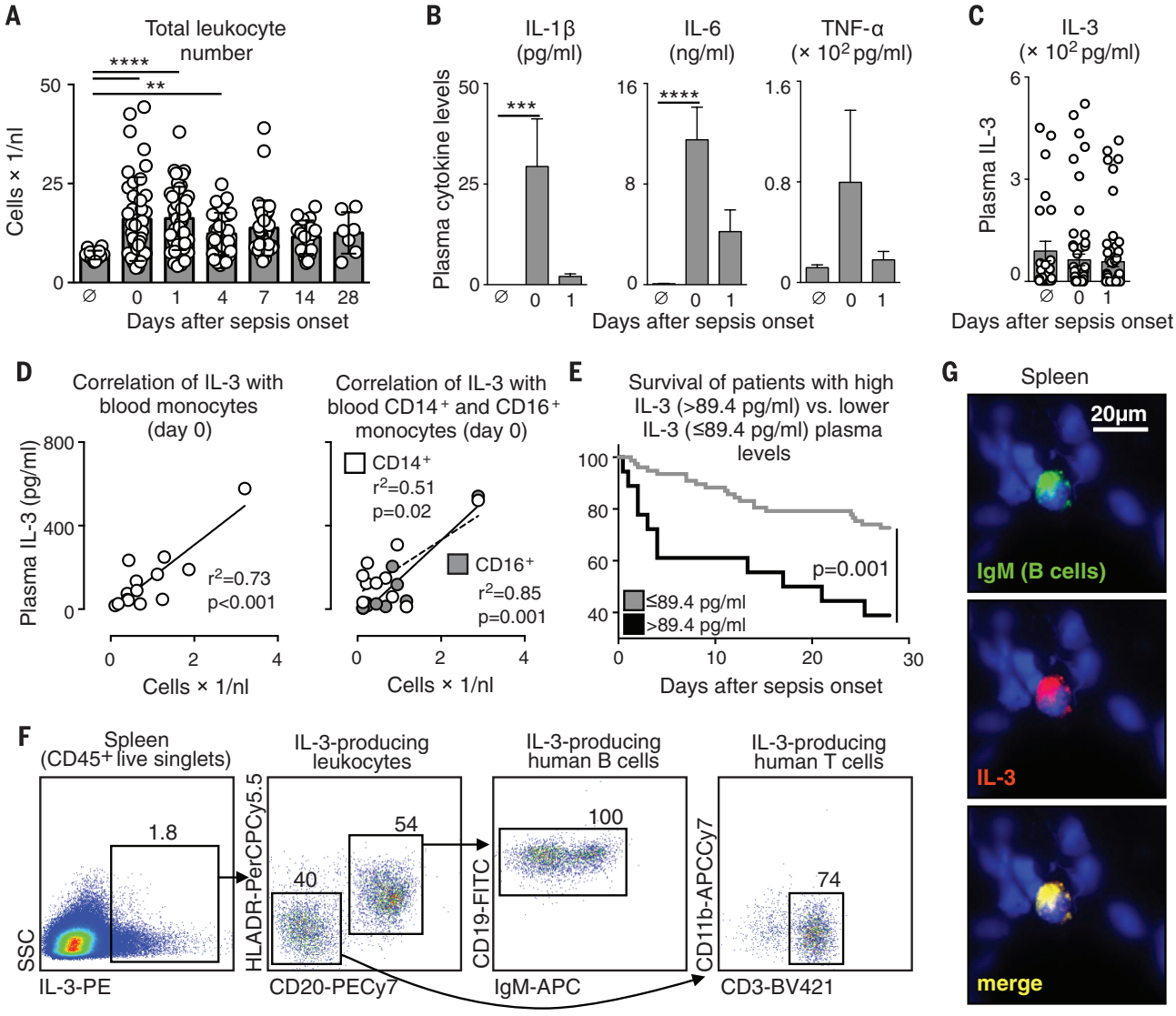

Fig. 4. IL-3 is an independent early predictor for outcome in human sepsis. (**A**) Total leukocyte number in nonseptic people and in septic patients at the time of sepsis onset (0) and 1, 4, 7, 14, and 28 days later. (**B**) Plasma levels of IL-1β, IL-6, and TNF-α in nonseptic people (n = 18) and in septic patients at the time of sepsis onset (n = 37) and 1 day later (n = 17). (**C**) IL-3 plasma levels in healthy people and in patients at sepsis onset and 1 day later. (**D**) Correlation of IL-3 plasma levels with total blood monocytes and with CD14$^+$ and CD16$^+$ blood monocytes in septic patients with measurable IL-3 plasma levels. (**E**) Kaplan-Meier analysis showing the survival of patients in the RAMMSES and SEPIL-3 studies with IL-3 at >89.4 pg/ml (top quintile, measured within 1 day after sepsis onset) versus the survival of patients with IL-3 ≤ 89.4 pg/ml. (**F**) Representative flow cytometry plot of n = 2 patients showing the identity of IL-3–producing human splenocytes. (**G**) Immunofluorescence of human spleen showing IL-3–producing B cells in high magnification (×60). A representative immunofluorescence section of n = 6 spleens is shown (*P < 0.05, ****P < 0.0001). Error bars indicate means ± SEM. Significance was assessed by one-way ANOVA with Tukey's multiple comparison test [(A) and (C)], a Pearson correlation test (D), and log rank (E). Data in (A) to (D) are from the SEPIL-3 cohort; data in (E) are pooled from the RAMMSES and SEPIL-3 cohorts.

amplify inflammation in humans as well as mice (fig. S15).

Mortality from sepsis ranges between 30 and 50% and is rising because of drug-resistant organisms, a growing elderly population, and an increased incidence of immunosuppression (*25*–*28*). The failures of anti–Toll-like receptor 4, recombinant activated protein C, and anti–TNF-α therapies in clinical trials necessitate a rethinking of sepsis' pathophysiology (*6*, *29*–*33*). Because many early-phase inflammatory cytokines operate concurrently and redundantly, identifying upstream triggers may generate therapies with broad downstream benefits. Altogether, the evidence shown here supports the hypothesis that IL-3 mediates experimental and human sepsis, is a major upstream orchestrator of the septic inflammatory phase, and can be harnessed for therapeutic intervention.

REFERENCES AND NOTES

1. Y. C. Yang *et al.*, *Cell* **47**, 3–10 (1986).
2. A. J. Hapel, J. C. Lee, W. L. Farrar, J. N. Ihle, *Cell* **25**, 179–186 (1981).
3. J. N. Ihle, L. Pepersack, L. Rebar, *J. Immunol.* **126**, 2184–2189 (1981).
4. G. T. Williams, C. A. Smith, E. Spooncer, T. M. Dexter, D. R. Taylor, *Nature* **343**, 76–79 (1990).
5. D. C. Angus, T. van der Poll, *N. Engl. J. Med.* **369**, 840–851 (2013).
6. R. S. Hotchkiss, G. Monneret, D. Payen, *Nat. Rev. Immunol.* **13**, 862–874 (2013).
7. C. S. Deutschman, K. J. Tracey, *Immunity* **40**, 463–475 (2014).
8. Materials and methods are available as supplementary materials on *Science* Online.
9. D. Rittirsch, M. S. Huber-Lang, M. A. Flierl, P. A. Ward, *Nat. Protoc.* **4**, 31–36 (2009).
10. M. C. Jamur, C. Oliver, *Front. Biosci. (Schol. Ed.)* **S3**, 1390–1406 (2011).
11. D. Voehringer, *Eur. J. Immunol.* **42**, 2544–2550 (2012).
12. E. Rönnberg *et al.*, *Immunology* **143**, 155–163 (2014).
13. D. Annane, E. Bellissant, J. M. Cavaillon, *Lancet* **365**, 63–78 (2005).
14. P. A. Ward, *EMBO Mol. Med.* **4**, 1234–1243 (2012).
15. M. Kondo *et al.*, *Annu. Rev. Immunol.* **21**, 759–806 (2003).
16. J. E. Groopman, J. M. Molina, D. T. Scadden, *N. Engl. J. Med.* **321**, 1449–1459 (1989).
17. A. H. Dalloul *et al.*, *Blood* **77**, 69–74 (1991).
18. P. J. Rauch *et al.*, *Science* **335**, 597–601 (2012).
19. G. F. Weber *et al.*, *J. Exp. Med.* **211**, 1243–1256 (2014).
20. I. Hilgendorf *et al.*, *Circulation* **129**, 1677–1687 (2014).
21. S. A. Ha *et al.*, *J. Exp. Med.* **203**, 2541–2550 (2006).
22. J. Seok *et al.*, *Proc. Natl. Acad. Sci. U.S.A.* **110**, 3507–3512 (2013).
23. K. Takao, T. Miyakawa, *Proc. Natl. Acad. Sci. U.S.A.* **112**, 1167–1172 (2015).
24. T. Brenner *et al.*, *Crit. Care* **18**, 683 (2014).
25. G. S. Martin, D. M. Mannino, S. Eaton, M. Moss, *N. Engl. J. Med.* **348**, 1546–1554 (2003).
26. K. A. Wood, D. C. Angus, *Pharmacoeconomics* **22**, 895–906 (2004).
27. M. Bosmann, P. A. Ward, *Trends Immunol.* **34**, 129–136 (2013).
28. C. M. Coopersmith *et al.*, *Crit. Care Med.* **40**, 1072–1079 (2012).
29. E. Dolgin, *Nat. Med.* **18**, 1000 (2012).
30. S. M. Opal *et al.*, *Crit. Care Med.* **25**, 1115–1124 (1997).
31. J. S. Boomer *et al.*, *JAMA* **306**, 2594–2605 (2011).
32. R. S. Hotchkiss, C. M. Coopersmith, J. E. McDunn, T. A. Ferguson, *Nat. Med.* **15**, 496–497 (2009).
33. P. A. Ward, *JAMA* **306**, 2618–2619 (2011).

ACKNOWLEDGMENTS

We thank M. Greene for secretarial assistance, M. Waring and A. Chicoine for sorting cells, and K. Joyes for editing the manuscript. The data presented in this manuscript are tabulated in the main paper and in the supplementary materials. The General Hospital Corporation has filed a patent application (61/973,458) with the U.S. Patent and Trademark Office entitled "Agents and Methods for Diagnosing and Treating Sepsis," which names F.K.S. and G.F.W. as inventors. *Il3*$^{-/-}$ mice are available from Riken, Japan, under a materials transfer agreement. This work was supported by NIH grants 5R01HL095612 and R56-AI104695 and the Massachusetts General Hospital Howard M. Goodman Fellowship (F.K.S.). G.F.W. was supported by the German Research Foundation (WE4892/1-2 and 3-1). B.G.C. was supported by the Société Française d'Anesthésie-Réanimation (SFAR), Institut Servier, Fondation Groupe Pasteur Mutualité, and Fulbright Scholarships (Monahan Foundation and Harvard French Scholarship Fund). M.N. was supported by an Erwin Schrödinger Fellowship of the Austrian Science Fund FWF (J3486-B13). The authors declare no conflicts of interest.

SUPPLEMENTARY MATERIALS

www.sciencemag.org/content/347/6227/1260/suppl/DC1
Materials and Methods
Figs. S1 to S15
Tables S1 to S6
References (*34*–*36*)

4 December 2014; accepted 21 January 2015
10.1126/science.aaa4268

CIRCADIAN RHYTHMS

Time-restricted feeding attenuates age-related cardiac decline in *Drosophila*

Shubhroz Gill,[1,2] Hiep D. Le,[1] Girish C. Melkani,[3]* Satchidananda Panda[1]*

Circadian clocks orchestrate periods of rest or activity and feeding or fasting over the course of a 24-hour day and maintain homeostasis. To assess whether a consolidated 24-hour cycle of feeding and fasting can sustain health, we explored the effect of time-restricted feeding (TRF; food access limited to daytime 12 hours every day) on neural, peripheral, and cardiovascular physiology in *Drosophila melanogaster*. We detected improved sleep, prevention of body weight gain, and deceleration of cardiac aging under TRF, even when caloric intake and activity were unchanged. We used temporal gene expression profiling and validation through classical genetics to identify the TCP-1 ring complex (TRiC) chaperonin, the mitochondrial electron transport chain complexes, and the circadian clock as pathways mediating the benefits of TRF.

To determine whether a daily rhythm of feeding and fasting without reducing caloric intake can improve health metrics, we subjected a 2-week-old wild-type (WT) Oregon-R strain (table S1) of *Drosophila melanogaster* adults to ad libitum feeding (ALF) or 12-hour time-restricted feeding (TRF) of a standard cornmeal diet exclusively during daytime. At nighttime, the TRF cohorts were placed in vials with 1.1% agar to prevent desiccation (fig. S1A). The daily food intake was equivalent in both groups, although ALF flies consumed some of their food during nighttime (Fig. 1A). Unlike ALF flies, the TRF group did not gain body weight at 5 and 7 weeks of age (Fig. 1B). The ability to fly (flight index) was slightly improved in the TRF group (Fig. 1C). Although the total daily activity was equivalent between both groups of flies (Fig. 1D), the TRF flies were more active during daytime. Sleep (defined as five consecutive minutes of inactivity) (*1*) assessment revealed that flies on TRF had less daytime sleep, but more nighttime and more total sleep, than the ALF flies (Fig. 1E and fig. S1).

Increase in sleep duration correlates with improved cardiac function (*2*). Therefore, by high-speed video imaging of ex vivo denervated hearts bathed in artificial hemolymph (*3*), we measured the diameter of the beating *Drosophila* heart at full relaxation and contraction and the time interval between successive contractions to calculate cardiac function parameters (Fig. 2A). At 3 weeks of age, the performance of both ALF and TRF hearts was indistinguishable with equivalent heart period (HP), systolic diameter (SD), systolic interval (SI), diastolic diameter (DD), diastolic interval (DI), arrhythmia index (AI), and heart contractility, measured as fractional shortening (FS) (Fig. 2, B to F; fig. S2; and movie S1). In the next 2 weeks, the cardiac performance in ALF flies exhibited characteristic age-dependent deterioration (*4*), with increased SI, DI, HP, and AI and reduced DD, SD, and FS. TRF flies showed smaller changes in these cardiac performance parameters in both genders (fig. S2).

We investigated whether a limited period of TRF early or late in life could attenuate age-dependent

[1]Regulatory Biology Laboratory, The Salk Institute for Biological Studies, La Jolla, CA 92037, USA. [2]Division of Biological Sciences, University of California San Diego, La Jolla, CA 92037, USA. [3]Department of Biology, Molecular Biology Institute, and Heart Institute, San Diego State University, San Diego, CA 92182, USA.
***Corresponding author. E-mail: gmelkani@mail.sdsu.edu (G.C.M.); satchin@salk.edu (S.P.)**

Interleukin-3 amplifies acute inflammation and is a potential therapeutic target in sepsis

Georg F. Weber *et al.*

Science **347**, 1260 (2015);
DOI: 10.1126/science.aaa4268